Sustainable Synthesis of Nickel Oxide Nanoparticles via *Manilkara Zapota* Extract for Advanced Wastewater Treatment

Prajapati Jay* and Patel K.N.
Department of Chemistry, Smt. M.G. Panchal Science College, Pilvai, 382850, INDIA
*jay97144@gmail.com

Abstract

Using leaf extract from Manilkara zapota, biogenic nickel oxide nanoparticles (NiO-NPs) were successfully produced and their photocatalytic effectiveness in breaking down Congo red dye was assessed. An eco-friendly, economical and sustainable substitute for traditional chemical processes is offered by this green synthesis technique. The structural, morphological and optical characteristics of the produced NiO-NPs were confirmed by means of Fourier Transform Infrared Spectroscopy (FTIR), UV-Vis spectroscopy, High-Resolution Transmission Electron Microscopy (HRTEM) and X-ray diffraction (XRD). NiO-NPs demonstrated strong photocatalytic activity when exposed to sunlight and important factors including catalyst dosage and dye concentration affected the rate of degradation. The degradation mechanism and ideal circumstances for maximum Congo red decolorization were determined, exposing the function of NiO-NPs in promoting redox reactions.

Furthermore, by lowering pH, electrical conductivity, chemical oxygen demand, total dissolved solids, phosphates and sulfates, NiO-NPs successfully enhanced wastewater quality. These results highlight the potential of biogenic NiO-NPs as an effective and environmentally benign remedy for environmental cleanup and azo dye degradation, supporting long-term pollution management plans.

Keyword: Photocatalytic degradation, Congo red dye, Green synthesis, Manilkara zapota extract, Wastewater treatment.

Introduction

Nickel oxide nanoparticles (NiO-NPs) have emerged as a prominent material in nanotechnology, captivating researchers with their exceptional chemical, physical, optical and biological properties. These characteristics make them highly versatile, leading to applications in catalysis, sensors, energy storage, biomedicine and environmental remediation[11]. They are also utilized in gas sensors, electrochromic films, magnetic materials and battery cathodes.

However, traditional techniques for creating NiO-NPs frequently call for dangerous chemicals, a lot of energy and may cause problems with biocompatibility[26]. The NPs thus lose their biological efficiency and biocompatibility[12]. As a result, biogenic synthesis is becoming more and more popular as a sustainable and environmentally friendly substitute[2].

Green synthesis, sometimes referred to as biogenic synthesis, is a bottom-up strategy that makes use of the stabilizing and reducing properties of natural biological resources. Because of their abundance, accessibility and intrinsic environmental friendliness, plant extracts, in particular, have drawn a lot of interest as efficient agents for the production of nanoparticles. The use of plant extracts offers several advantages including simplicity, cost-effectiveness, reduced toxicity and the potential for large-scale production[7,17]. Additionally, significant antibacterial, antioxidant, anticancer and anti-inflammatory qualities have been shown by green produced NiO-NPs[9].

The photocatalytic degradation of organic pollutants such as Congo red dye, is a crucial area of research for addressing environmental pollution. The textile, leather, paper and food sectors all make substantial use of azo dyes, which are distinguished by the presence of one or more azo (-N=N-) groups. Because NiO-NPs may effectively be used to remove both organic and inorganic contaminants, they are essential for protecting the environment[7]. NiO-NPs, with their semiconductor properties and high surface area, exhibit excellent photocatalytic activity, enabling the degradation of organic dyes under light irradiation[14].

This research focuses on the synthesis of NiO-NPs using *Manilkara zapota* leaf extracts and evaluates their effectiveness in the photocatalytic degradation of congo red dye. *Manilkara zapota*, known for its medicinal properties and rich phytochemical composition, is used as a reducing and stabilizing agent. The synthesized NiO-NPs are characterized using various techniques to confirm their formation, morphology and crystalline structure. By analysing the impact of different parameters such as catalyst loading, dye concentration, pH and light intensity on the degradation efficiency of congo red, the study explores the photocatalytic activity of the biogenic NiO-NPs.

The potential of NiO-NPs for industrial wastewater treatment is also explored, highlighting their role in reducing key pollution indicators. By proposing a viable path toward resource conservation and pollution reduction, this study seeks to shed light on the sustainable synthesis and use of NiO-NPs for environmental remediation.

Material and Methods

Material: All materials used in this study were of analytical grade and were utilized without further purification. Nickel nitrate hexahydrate [$Ni(NO_3)_2 \cdot 6H_2O$] was procured from HI MEDIA, India and served as the nickel source. *Manilkara zapota* leaves were obtained from a botanical garden Smt M.G. Panchal Science College, Pilvai (Gujarat), India. The Congo red dye used in the experiments was supplied by SD Fine Chemicals Ltd. Other reagents, including sodium hydroxide (NaOH) and hydrochloric acid (HCl) for pH adjustment, were obtained from Merck India. Deionized water was used for all solution preparations. All glassware and instruments were thoroughly cleaned and sterilized before use to ensure the accuracy and reliability of experimental results.

Plant extract synthesis: After being gathered, fresh *Manilkara zapota* leaves were carefully cleaned to get rid of any dirt and allowed to dry in the shade for about two weeks. A fine powder was then created by crushing the dried leaves. The extract was made by heating 5.0 g of the powdered leaves with 50 mL of Milli-Q water at 80 °C for an hour while stirring constantly. After cooling to room temperature, the mixture was filtered using 0.45 µm Whatmann filter paper to remove any solid residues. The resulting brown-colored leaf extract was stored at 4 °C overnight and used for the synthesis of NiO-NPs[21].

Synthesis of Nickel oxide nanoparticles: Nickel oxide nanoparticles (NiO-NPs) were synthesized using *Manilkara zapota* leaf extract. First, fresh leaves were dried, grind into a fine powder and extracted with Milli-Q water at 80°C. After filtering, the extract was kept for later use. 2.4 grams of nickel(II) nitrate hexahydrate were dissolved in 100 millilitres of distilled water to create a nickel precursor solution. After adding 1 M NaOH and the plant extract in a 1:1 ratio, the mixture was constantly stirred for an hour at 70°C to 80°C. After centrifuging the resultant mixture, the precipitate was repeatedly cleaned with ethanol and distilled water. To create NiO nano powder, the collected precipitate was first dried in an oven at 240°C and then calcined for four hours at 500°C[22].

Characterization: A Systronics UV-VIS Spectrophotometer 117-TS was used to capture UV-visible absorbance spectra in order to track the organic dye's degradation. Functional group analysis was performed using a Shimadzu-8400 FTIR spectrometer, with 100 scans recorded in the 4000−400 cm^{-1} range (Vaibhav Analytical Lab, Ahmedabad, Gujarat, India). The crystallinity and phase structure of the synthesized NiO-NPs were analyzed by X-ray diffraction (XRD) using a Miniflex Rigaku-600 instrument at 30 kV and 2 mA, with a scan speed of 10.0° min^{-1}, employing a Cu-Kα radiation source and a graphite monochromator. The powder samples were scanned in continuous mode across a 2θ range of 3–90° (CIMF Lab, Department of Chemistry, HNGU, Patan, Gujarat, India). High-Resolution Transmission Electron Microscopy (HRTEM) was performed using a Field Emission Gun-Transmission Electron Microscope (FEG-TEM, 300 kV, Sophisticated Analytical Instrumentation Facility, Panjab University, Chandigarh) to analyze the shape, size and morphology of NiO NPs as well as their crystallinity through selected area electron diffraction (SAED) patterns.

Photocatalytic activity: In this study, advanced oxidation processes (AOPs) were employed to investigate the photocatalytic degradation of congo red dye using NiO-NPs as the oxidant. Reaction parameters including pH and light intensity were carefully regulated while dye solutions were made in deionized water. A 20 mL dye solution (60 ppm) with 5 mg of NiO photocatalyst was maintained at pH 4 and exposed to sunlight, with intensity measured using a digital Lux meter. At 30-minute intervals, samples were centrifuged and absorbance at 497 nm was recorded using a UV-Vis spectrophotometer to monitor the degradation rate.

The reaction followed pseudo-first-order kinetics, as confirmed by the linear plot of 2 + log O.D, with the rate constant (k) calculated from the slope.

The study examined the effects of dye concentration, pH and photocatalyst dosage, establishing the optimal degradation conditions: 60 ppm dye concentration, pH 4 and 5 mg NiO-NPs. The results confirmed the necessity of photocatalyst, oxygen and light for effective degradation, demonstrating NiO-NPs's potential for dye removal in wastewater treatment.

Results and Discussion

UV-Visible spectroscopy: UV-visible spectroscopy was used to examine the optical characteristics of the produced NiO-NPs in the 200–800 nm range. A large absorption peak with a centre at 330 nm was visible in the absorbance spectra shown in figure 1, which is characteristic of NiO-NPs[1]. This peak arises due to the intrinsic electronic transitions of Ni^{2+} ions in the NiO lattice, specifically from the charge transfer transitions between O^{2-} and Ni^{2+}. The observed absorption peak slightly deviates from the reported values for bulk NiO, indicating the nanoscale nature of the synthesized particles.

The broadness of the peak suggests polydispersity and possible surface defects, which can influence the bandgap energy. The presence of minor fluctuations or noise in the spectrum could be attributed to light scattering by the NPs and surface plasmon resonance effects. The optical bandgap of NiO-NPs can be further analyzed using Tauc's plot, which provides insight into their semiconductor nature. A quantum confinement effect, which is frequently seen in nanostructured materials, is suggested by the blue shift in the absorption edge when compared to bulk NiO, which is normally approximately 360–380 nm[26]. These optical properties confirm that the synthesized NiO-NPs are suitable for photocatalytic applications, as they efficiently absorb UV light, making them potential candidates for environmental remediation and dye degradation processes.

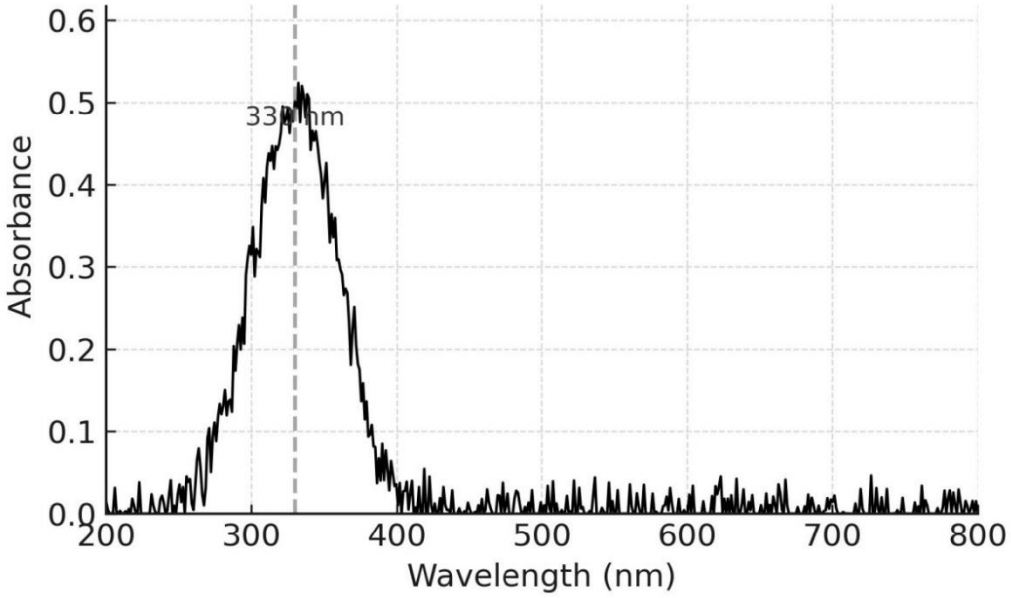

Figure 1: UV-Visible spectrum of NiO-NPs

The existence of distinctive peaks in the UV-Vis spectrum indicates that NiO-NPs have formed. A surface plasmon resonance (SPR) band is visible in NiO-NPs, albeit the precise wavelength varies according on the NPs' size, shape and surroundings. Changes in SPR band's position (wavelength) and intensity can indicate size and concentration of synthesized NPs. A sharper, more intense peak generally indicates smaller, more uniform NPs. Fe_2O_3 NPs synthesized using plant extracts have shown SPR bands around 344-355 nm[25]. The SPR band for silver nanoparticles (AgNPs) was detected at 390 nm in the green synthesis of AgNPs utilizing leaf extract from *Manilkara zapota*[3]. The extract will show a complex spectrum related to its various phytochemicals, while the NiO-NPs will exhibit a characteristic SPR band that confirms their formation and provides information about their size and optical properties.

X-ray Diffraction Spectroscopy (XRD): The XRD spectrum of the synthesized material exhibits distinct peaks of diffraction at 2θ values of approximately 37°, 43°, 62.7°, 75.5° and 79.1° as shown in figure 2. The (111), (200), (220), (311) and (222) crystallographic planes are represented by these peaks respectively. The presence of these peaks confirms the formation of a crystalline NiO phase. The peak positions match well with the standard reference pattern for NiO, indicating that the synthesized material is indeed nickel oxide. The produced NiO-NPs appear to be well-crystallized based on the strength and clarity of the diffraction peaks. Higher intensity indicates a higher degree of crystallinity.

The Scherrer equation, which links peak broadening to crystallite size, can be used to estimate the average crystallite size. The degree of broadening of the peaks indicates that the NiO particles are in the nanometer range. The XRD pattern's lack of extra peaks suggests that the produced NiO-NPs are comparatively clean and free of crystalline impurities[8,15]. In summary, the XRD analysis confirms the successful synthesis of crystalline and relatively pure NiO-NPs. The spectrum indicates a face-centered cubic structure and suggests that the particles are in the nanometer range[5].

Fourier Transform Infrared Spectroscopy (FTIR): The FTIR spectrum of the *Manilkara zapota* plant extract exhibits several notable absorption bands, as shown in figure 3. Around 3300 cm^{-1}, a large, strong absorption band is seen, signifying the presence of O-H stretching vibrations, which are typical of carboxylic acids, alcohols and phenols. This implies that the plant extract contains hydroxyl groups, most likely as a result of water content or the presence of phenolic or alcoholic chemicals[19]. Smaller peaks appear around 2900 cm^{-1} corresponding to C-H stretching vibrations, which are commonly found in alkanes and other organic molecules, indicating the presence of aliphatic compounds.

Moreover, C=O stretching vibrations, which are typical of carbonyl-containing compounds such as aldehydes, ketones, carboxylic acids and esters, are responsible for a group of tiny peaks that lie between 1600 and 1700 cm^{-1}. This suggests the presence of these functional groups in the plant extract. Furthermore, a peak around 1000 cm^{-1} corresponds to C-O stretching vibrations which are typically associated with alcohols, ethers and polysaccharides, indicating the presence of carbohydrates or other ether-containing compounds.

In summary, the FTIR spectrum of *Manilkara zapota* extract reveals the presence of hydroxyl (O-H), alkane (C-H), carbonyl (C=O) and ether or alcohol (C-O) functional groups. These groups highlight the complex mixture of phytochemicals in the extract contributing to its reducing and stabilizing properties in NPs synthesis[4].

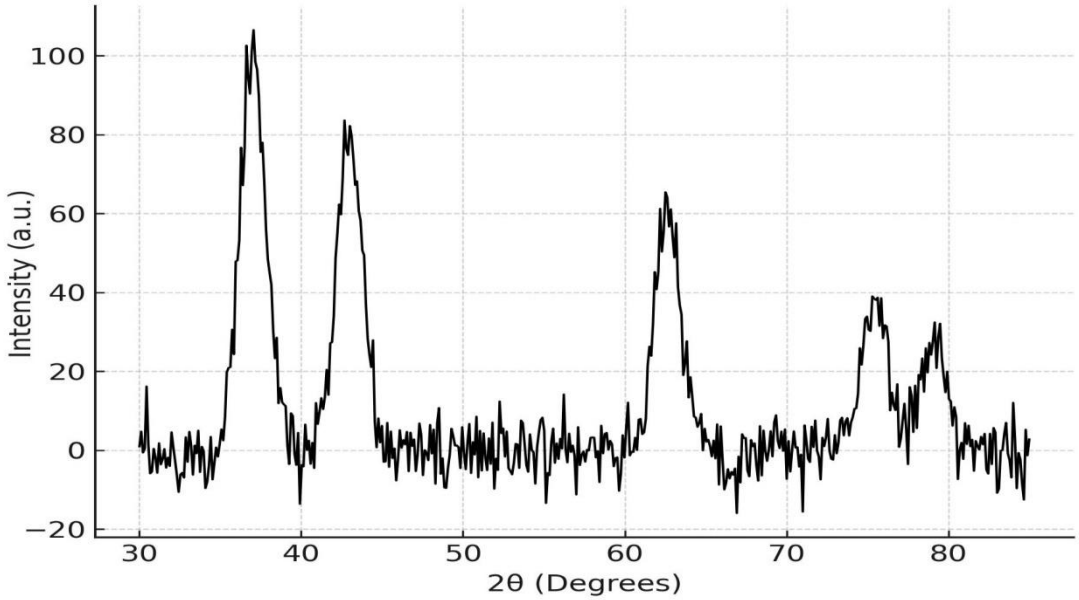

Figure 2: XRD Spectrum of NiO-NPs

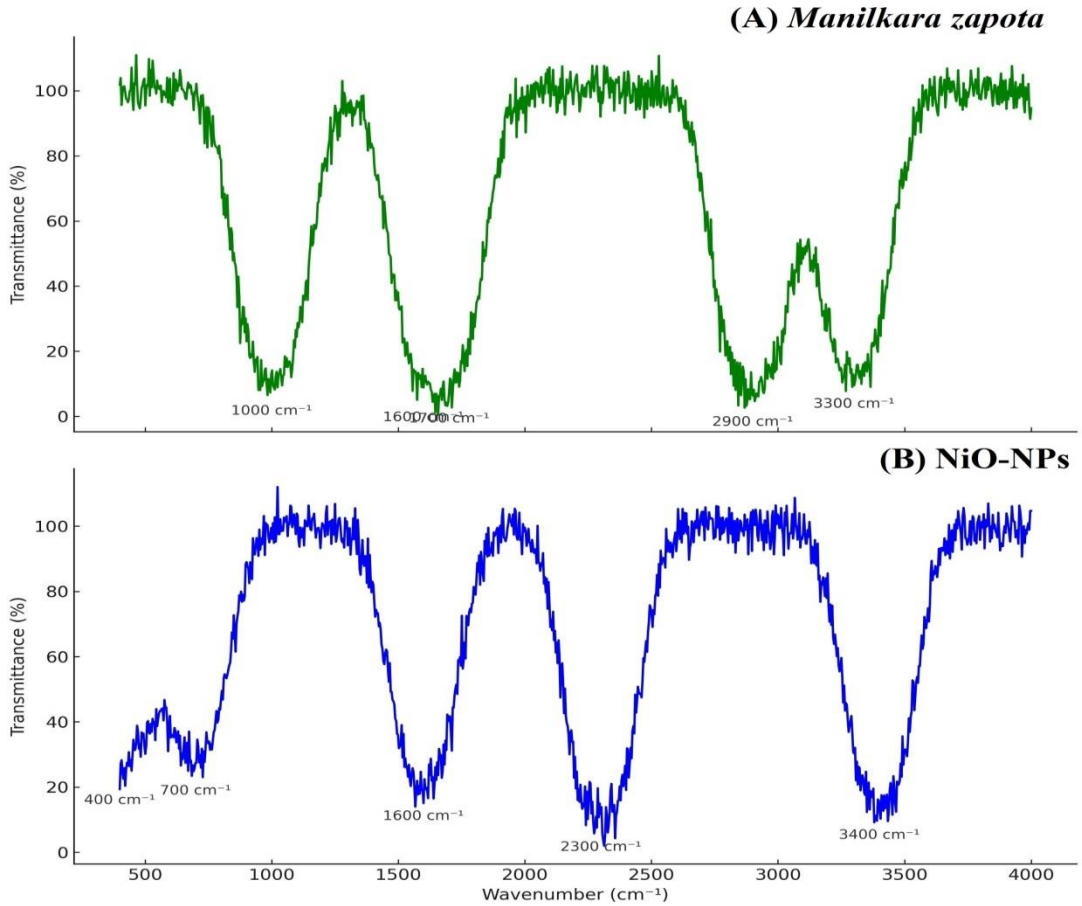

Figure 3: FTIR spectrum of *Manilkara zapota* and NiO-NPs

Likewise, figure 3 representation of the NiO-NPs FTIR spectrum reveals distinctive absorption bands. Because of the O-H stretching vibrations of alcohols, phenols and carboxylic acids, a large absorption band is seen at about 3400 cm^{-1}, suggesting the presence of surface-adsorbed water molecules or -OH groups on the NiO-NPs surface[24]. Small peaks around 2300 cm^{-1} are present which could be attributed to background noise or the presence of CO_2. An absorption band near 1600 cm^{-1} may be related to adsorbed CO_2 and confirms the existence of carbonyl groups' C=O stretching vibrations. With absorption bands below 700 cm^{-1}, multiple peaks in the 1400–400 cm^{-1} area are seen, indicating the presence of Ni-O stretching vibrations as a sign of NiO production[11].

The FTIR spectrum thus confirms the synthesis of NiO-NPs, revealing a face-centered cubic structure. Additionally, the observed surface hydroxyl groups may influence the physicochemical properties of the NiO-NPs.

High-Resolution Transmission Electron Microscopy (HR-TEM): The size, shape and structural properties of the produced NiO-NPs were ascertained by means of an examination using High-Resolution Transmission Electron Microscopy (HR-TEM). Figures 4 (A) and (B) display the HR-TEM micrographs which show the morphology and 4(C) the particle size distribution of the NPs[20]. As shown in figure 4(A), the NiO-NPs exhibit a tendency to form small agglomerates due to Van der Waals interactions. Individual particles within the agglomerates appear to be nearly spherical, with a few exhibiting slight distortions. The well-defined, high-contrast image in figure 4(B) further confirms the formation of NiO-NPs with a crystalline nature, as shown by the lattice fringes seen in high-resolution pictures.

The particle size distribution histogram in figure 4(C) indicates that the average particle size is between 15 and 40 nm, with a predominant size of 25 to 30 nm. NiO-NPs' consistent size distribution and distinct shape point to a successful synthesis with regulated nucleation and growth. The high electron density observed in the HR-TEM images is characteristic of metal oxide nanoparticles. The presence of faceted nanoparticles in figure 4(B) suggests a polycrystalline nature, likely due to the thermodynamically favored crystal growth of NiO. Additionally, the size distribution analysis in figure 4(C) follows a Gaussian distribution, indicating uniformity in particle growth.

The HR-TEM analysis confirms the successful synthesis of NiO-NPs with a nearly spherical morphology and a particle size range of 15–40 nm. The presence of well-defined nanoparticles with a uniform distribution suggests the efficacy of the synthesis method in producing NiO-NPs with controlled size and morphology[16].

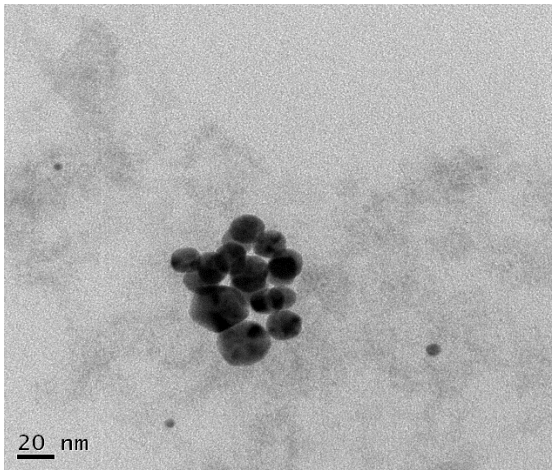

Figure 4(A)

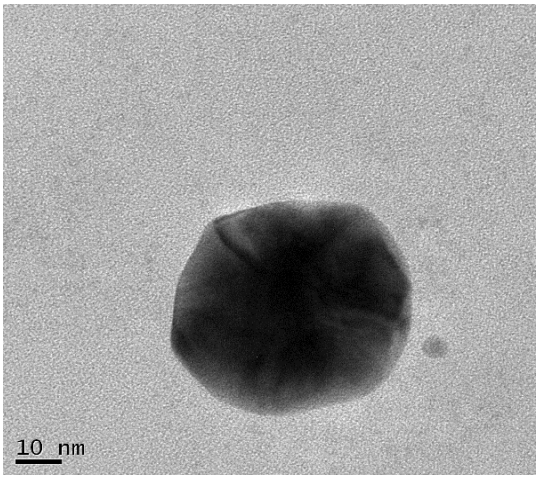

Figure 4(B)

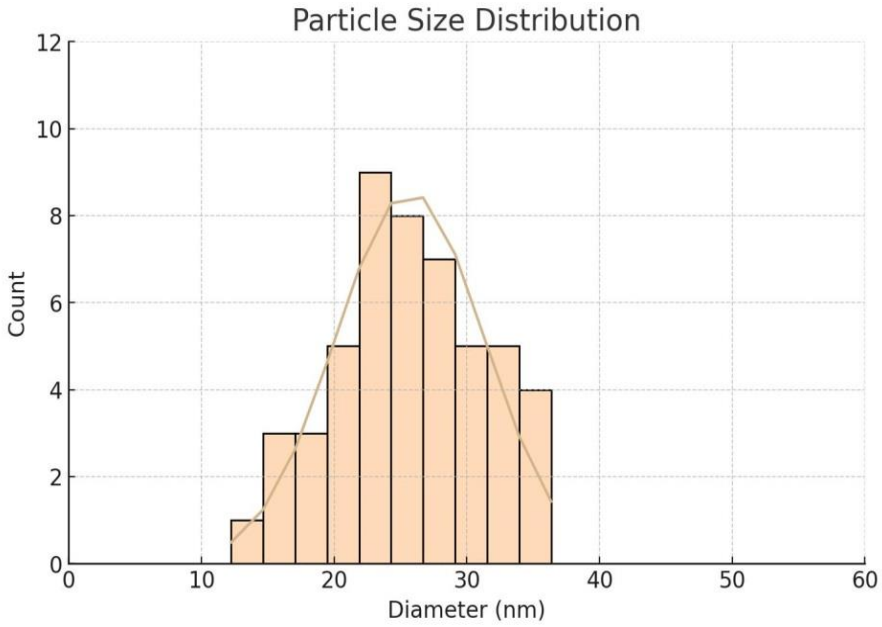

Figure (C)

Figure 4: (A, B) HR-TEM Images of NiO-NPs and (C) NPs Size Distribution Curve

Effect of Dye Concentration: Congo red dye's photocatalytic breakdown was examined at different starting concentrations (20–80 ppm) while keeping the following constants: pH 3.12 and a 5 mg NiO dose[10]. To track the deterioration process, the absorbance values at 497 nm were taken at regular intervals. The results of table 1 indicate that as the dye concentration increases, the degradation rate decreases. For lower concentrations (20-40 ppm), a significant reduction in absorbance is observed within the first 180 minutes, suggesting faster degradation. At 20 ppm, the optical density (O.D) decreases from 0.491 to 0.180 over 180 minutes, indicating efficient breakdown of the dye molecules. Similarly, for 30 ppm and 40 ppm, the absorbance reduces to 0.189 and 0.393 respectively, demonstrating effective degradation. At higher concentrations (50-80 ppm), the rate of degradation slows down, likely due to excessive dye molecules limiting the penetration of light and hindering photocatalytic activity. For 60 ppm, the absorbance drops from 1.123 to 0.210 after 180 minutes whereas at 80 ppm, the degradation is significantly lower, with the O.D. reducing from 2.088 to 1.275. According to this pattern, there is an ideal dye concentration for efficient photocatalytic degradation, over which the efficiency declines.

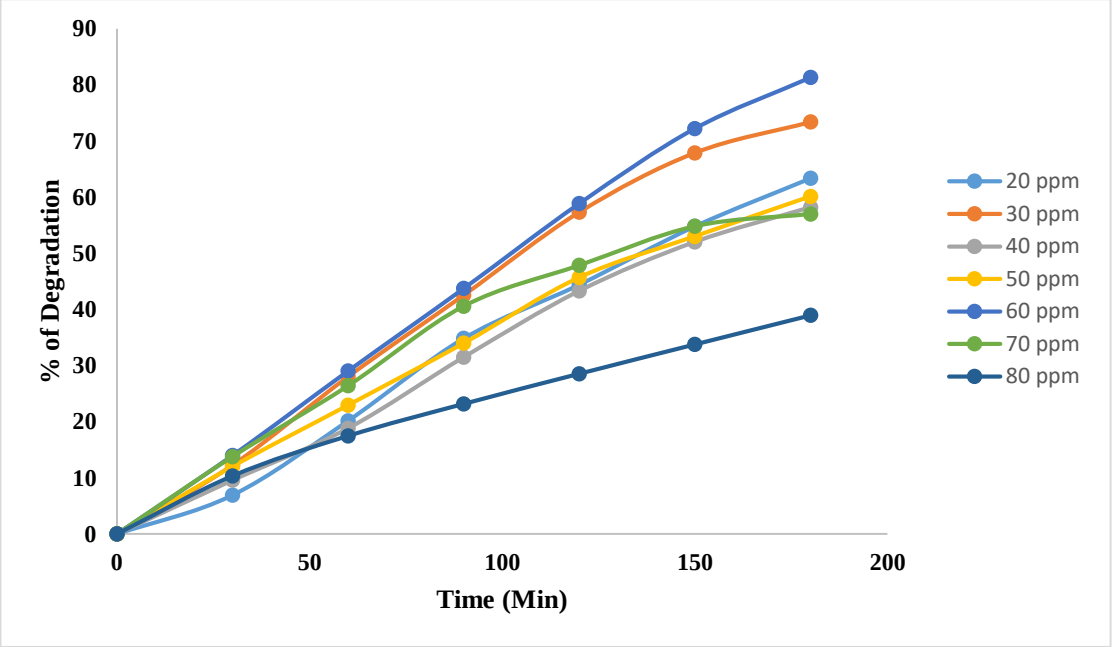

Figure 5: Effect of Initial Congo Red Dye Concentration on Photocatalytic Degradation Using NiO-NPs

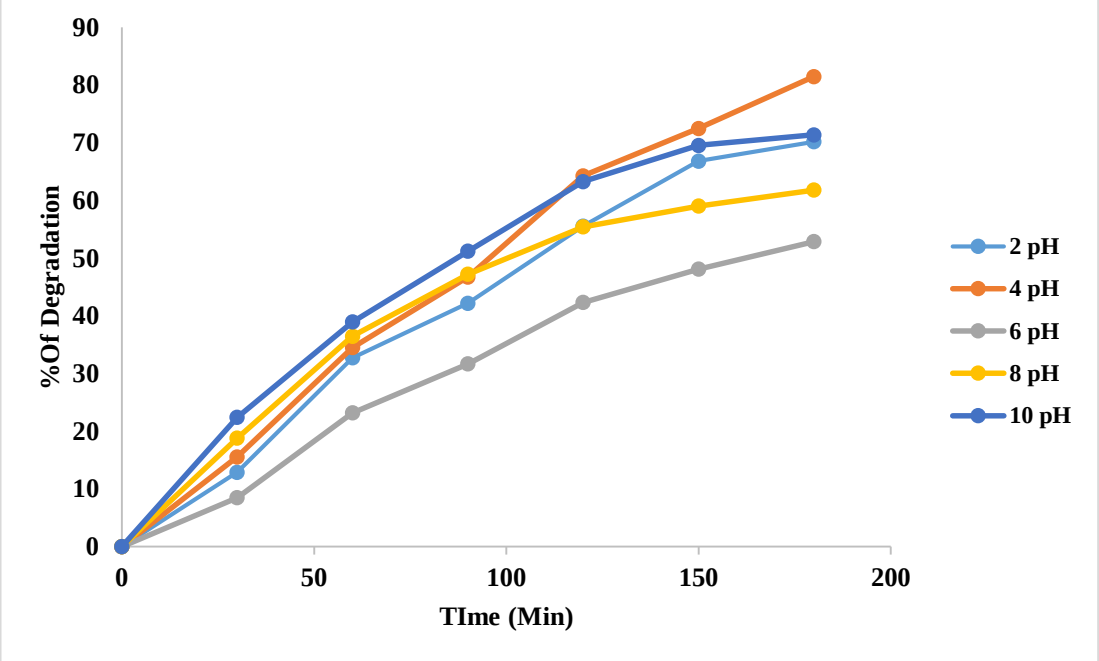

Figure 6: Effect of pH on % Degradation of Congo Red

Figure 5 represented effect of concentration of Congo red dye on percentage degradation of Congo red dye However, the information demonstrates that pseudo-first-order kinetics governed the degradation as observed from the steady decline in absorbance over time. The reduction in O.D with increasing reaction time signifies a decrease in dye concentration due to NiO NPs' catalytic activity. Better light penetration and greater active site availability on NiO-NPs are responsible for the improved degradation at lower concentrations[6]. Conversely, the degradation efficiency is probably limited at greater concentrations by decreased light absorption and charge carrier recombination. Overall, the study demonstrates that NiO-NPs effectively degrade congo red dye, with optimal degradation occurring at lower dye concentrations. These findings highlight the potential of NiO as a photocatalyst for wastewater treatment applications.

Effect of pH: At various pH values between 2 and 10, the degradation efficiency of congo red dye by NiO-NPs was examined while keeping the dye concentration constant at 60 ppm and the NiO dosage at 5 mg. Table 2 illustrates the results which showed that pH had a substantial impact on the rate of degradation. At highly acidic conditions (pH 2), the initial absorbance was recorded at 1.519 which gradually decreased to 0.453 after 180 minutes. A similar trend was observed at pH 4 where the absorbance dropped from 1.408 to 0.261, indicating a higher degradation rate compared to pH 2. The most effective degradation occurred at pH 10, with a substantial decrease in absorbance from 0.660 to 0.189 within the same time frame. This suggests that alkaline conditions favor enhanced photocatalytic activity of NiO, leading to rapid dye degradation[18].

On the other hand, at neutral pH (pH 6) and slightly alkaline conditions (pH 8), the dye degradation rate was relatively slower. The absorbance decreased from 1.566 to 0.738 at pH 6 and from 1.330 to 0.508 at pH 8, indicating moderate degradation efficiency. The decreased availability of hydroxyl radicals, which are essential for oxidative degradation, may be the cause of the decreased degradation efficiency at pH 6.

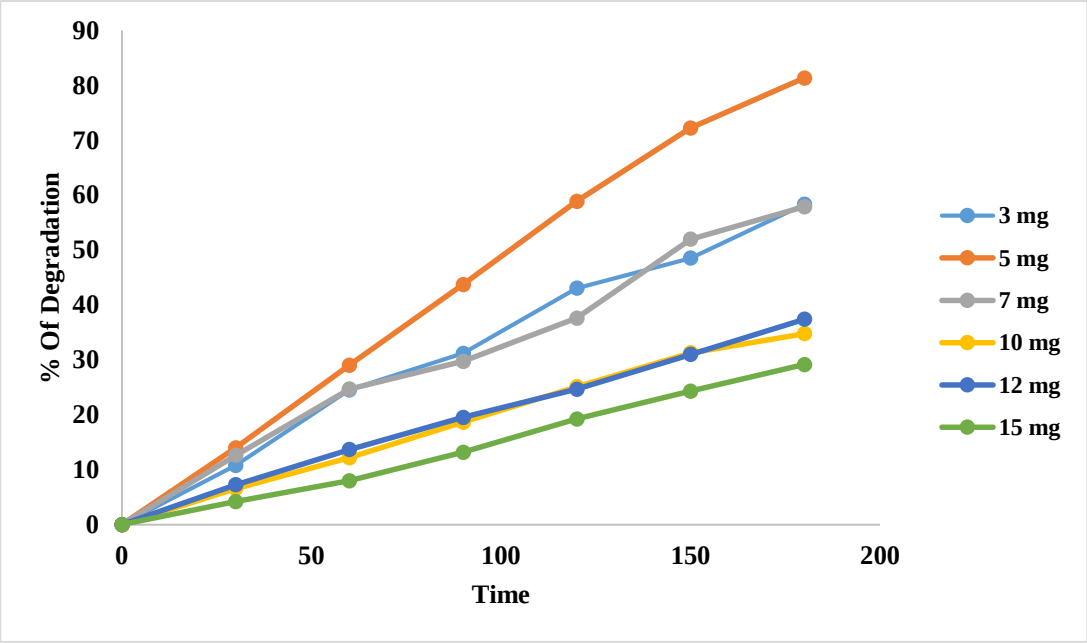

Figure 7: Effect of NiO NPs on % Degradation of Congo Red dye

Table 1
Effect of Initial Congo Red Dye Concentration on Photocatalytic Degradation using NiO-NPs (Absorbance values measured at 497 nm over different time intervals at pH 3.12, NiO dosage of 5 mg)

	Concentration of Congo Red Dye						
Time (Min.)	**20 ppm**	**30 ppm**	**40 ppm**	**50 ppm**	**60 ppm**	**70 ppm**	**80 ppm**
	Percentage of Photocatalytic Degradation						
0	0	0	0	0	0	0	0
30	6.924	12.253	9.574	12.024	13.980	13.779	10.345
60	20.163	28.028	18.829	22.946	29.029	26.400	17.480
90	34.827	42.535	31.489	33.967	43.722	40.566	23.180
120	44.399	57.323	43.298	45.691	58.860	47.842	28.544
150	54.786	67.887	52.021	53.006	72.217	54.797	33.764
180	63.340	73.380	58.191	60.120	81.300	56.986	38.937

Table 2
Effect of pH of solution on Photocatalytic Degradation using NiO-NPs (Volume of Dye = 60 ppm, Amount of NiO = 5 mg, pH = 2 – 10

	pH of solution				
Time (Min.)	**pH 2**	**pH 4**	**pH 6**	**pH 8**	**pH 10**
	Percentage of Photocatalytic Degradation				
0	0	0	0	0	0
30	12.903	15.554	8.492	18.797	22.424
60	32.719	34.517	23.180	36.466	38.939
90	42.199	46.733	31.673	47.218	51.212
120	55.563	64.276	42.337	55.413	63.281
150	66.820	72.463	48.084	59.022	69.545
180	70.178	81.463	52.873	61.804	71.363

Table 3
Effect of amount of NiO-NPs on Photocatalytic Degradation using NiO-NPs (Volume of Dye = 60 ppm, Amount of NiO NPs = 3 - 12 mg, pH = 3.12,

	Amount of NiO NPs					
Time (Min.)	**3 mg**	**5 mg**	**7 mg**	**10 mg**	**12 mg**	**15 mg**
	Percentage of Photocatalytic Degradation					
0	0	0	0	0	0	0
30	10.781	13.980	12.601	6.536	7.237	4.185
60	24.528	29.029	24.663	12.180	13.670	7.989
90	31.177	43.722	29.717	18.657	19.529	13.152
120	43.037	58.860	37.601	25.074	24.641	19.239
150	48.518	72.217	51.954	31.254	30.959	24.293
180	58.311	81.300	57.884	34.759	37.392	29.130

Figure 6 represented effect of pH on percentage degradation of Congo red dye However, the results confirm that the photocatalytic activity of NiO-NPs is strongly dependent on pH, with optimal degradation occurring under alkaline conditions. Higher pH levels cause more hydroxyl radicals to be produced, which speeds up the breakdown of the dye molecules and accounts for the increased degradation[23]. These findings highlight the importance of pH control in optimizing photocatalytic processes for wastewater treatment applications.

Effect of NiO-NPs: A fixed dye concentration of 60 ppm and pH 3.12 under solar irradiation were used to test the effects of different NiO-NPs concentrations (3 mg to 15 mg) on the photocatalytic degradation of congo red dye. The results (Table 3) demonstrate that the amount of NiO plays a crucial role in the degradation process. At a lower catalyst concentration (3 mg), the absorbance decreased from 1.113 to 0.464 after 180 minutes, indicating a moderate degradation rate. As the amount of NiO increased to 5 mg, a significant improvement in dye degradation was observed, with the absorbance reducing from 1.123 to 0.210, suggesting enhanced photocatalytic efficiency. The enhanced availability of active sites for dye adsorption and subsequent degradation is responsible for this improvement[28]. Figure 7 represented effect of NiO-NPs on percentage degradation of congo red dye. However, as the NiO concentration was further increased to 7 mg, 10 mg and beyond, the degradation rate started to decline. At 12 mg and 15 mg, the final absorbance values after 180 minutes were 1.090 and 1.304 respectively[13], indicating reduced photocatalytic efficiency. This reduction in degradation efficiency at higher NiO concentrations may be due to excessive catalyst loading, leading to agglomeration and decreased surface area available for photocatalysis. Additionally, higher concentrations may cause light scattering and shading effects, reducing the effective penetration of light into the reaction medium.

These findings suggest that 5 mg of NiO is the optimal catalyst concentration for maximum congo red dye degradation under the given experimental conditions. Beyond this concentration, further increases in catalyst dosage do not contribute to improved degradation efficiency and may even hinder the photocatalytic process[27].

Conclusion

The synthesis and characterization of NiO-NPs were successfully carried out and their photocatalytic properties were evaluated. The creation of NiO-NPs with a distinctive absorption peak at 330 nm, demonstrating their nanoscale nature and quantum confinement effects, was confirmed by the UV-visible spectroscopic investigation. The face-centered cubic structure with an average crystallite size in

the nanometer range was shown by the XRD examination which further confirmed the crystalline nature of the NiO-NPs. The presence of functional groups that aid in the stability and production of NiO-NPs, was verified by the FTIR analysis. The nanoparticles' homogeneous size distribution and almost spherical shape, with an average particle size between 15 and 40 nm, were shown by HR-TEM imaging.

The effectiveness of NiO-NPs in wastewater treatment applications was demonstrated by the photocatalytic degradation tests of congo red dye. Numerous factors such as the initial dye concentration, pH and the quantity of NiO-NPs, were shown to affect the degradation rate. Optimal degradation occurred at lower dye concentrations (20–40 ppm) due to enhanced light penetration and active site availability. The study also revealed that alkaline conditions (pH 10) favored maximum photocatalytic activity due to the increased generation of hydroxyl radicals. Additionally, the effect of NiO-NPs concentration showed that an optimal dosage (5 mg) provided the highest degradation efficiency, while excessive nanoparticle loading led to reduced photocatalytic performance due to particle aggregation and reduced light absorption.

All things considered, these results show that NiO-NPs have outstanding photocatalytic qualities, which makes them attractive options for environmental remediation, especially in applications involving dye degradation. Future studies can focus on optimizing reaction conditions, exploring hybrid nanostructures and evaluating the recyclability of NiO-NPs to enhance their practical applicability in wastewater treatment.

Acknowledgement

We would like to express our sincere gratitude to M.G. Panchal Science College Pilvai and Hemchandracharya North Gujarat University for their support and encouragement throughout this research. We deeply appreciate the valuable resources and guidance of staff members of M.G. Panchal Science College, Pilvai.

References

1. Aarthi J. et al, Green synthesis and characterization of NiO nanoparticles using Catharanthus roseus leaf extract, Materials Today: Proceedings, **69**, 1455-1461 **(2022)**

2. Absi E., Saleh M., Al-Hada N.M., Hamzah K., Alhawsawi A.M. and Banoqitah E.M., A review on preparation and characterization of silver/nickel oxide nanostructures and their applications, *Applied Physics A*, **127**, 1-32 **(2021)**

3. Ali T. et al, Green nickel/nickel oxide nanoparticles for prospective antibacterial and environmental remediation applications, *Ceramics International*, **48(6)**, 8331-8340 **(2022)**

4. Al-Zaqri N., Umamakeshvari K., Mohana V., Muthuvel A. and Boshaala A., Green synthesis of nickel oxide nanoparticles and its photocatalytic degradation and antibacterial activity, *Journal of Materials Science: Materials in Electronics*, **33(15)**, 11864-11880 **(2022)**

5. Balto H., Amina M., Bhat R.S., Al-Yousef H.M., Auda S.H. and Elansary A., Green synthesis of nickel nanoparticles using Salvadora persica and their application in antimicrobial activity against oral microbes, *Microbiology Research*, **14(4)**, 1879-1893 **(2023)**

6. Ben Ayed S., Azam M., Al-Resayes S.I., Ayari F. and Rizzo L., Cationic dye degradation and real textile wastewater treatment by heterogeneous photo-fenton, using a novel natural catalyst, *Catalysts*, **11(11)**, 1358 **(2021)**

7. Berhe M.G. and Gebreslassie Y.T., Biomedical applications of biosynthesized nickel oxide nanoparticles, *International Journal of Nanomedicine*, **18**, 4229-4251 **(2023)**

8. Bhoye M. et al, Eco-friendly synthesis of Ni/NiO nanoparticles using Gymnema Sylvestre leaves extract for antifungal activity, Journal *of Composites Science*, **7(3)**, 105 **(2023)**

9. Danjumma S.G., Abubakar Y. and Suleiman S., Nickel oxide (NiO) devices and applications: a review, *J. Eng. Res. Technol*, **8**, 12-21 **(2019)**

10. Dihom H.R., Al-Shaibani M.M., Mohamed R.M.S.R., Al-Gheethi A.A., Sharma A. and Khamidun M.H.B., Photocatalytic degradation of disperse azo dyes in textile wastewater using green zinc oxide nanoparticles synthesized in plant extract: A critical review, *Journal of Water Process Engineering*, **47**, 102705 **(2022)**

11. Hazra K., Dutta S., Paria D., Ghosal S. and Rao M.M., Phytopharmacognostical profile of Manilkara zapota (L.) P. Royen seeds, *Journal of Pharmacognosy and Phytochemistry*, **8(4)**, 3038-3043 **(2019)**

12. Huang Y.W., Cambre M. and Lee H.J., The toxicity of nanoparticles depends on multiple molecular and physicochemical mechanisms, *International Journal of Molecular Sciences*, **18(12)**, 2702 **(2017)**

13. Khan S., Noor T., Iqbal N. and Yaqoob L., Photocatalytic dye degradation from textile wastewater: a review, *ACS Omega*, **9(20)**, 21751-21767 **(2024)**

14. Khodair Z.T., Ibrahim N.M., Kadhim T.J. and Mohammad A.M., Synthesis and characterization of nickel oxide (NiO) nanoparticles using an environmentally friendly method and their biomedical applications, *Chemical Physics Letters*, **797**, 139564 **(2022)**

15. Mandal B.K. et at, Green synthesis of NiO nanoparticle using Punica granatum peel extract and its characterization for methyl orange degradation, Materials Today Communications, **34**, 105302 **(2023)**

16. Moghadam N.C.Z., Jasim S.A., Ameen F., Alotaibi D.H., Nobre M.A., Sellami H. and Khatami M., RETRACTED ARTICLE: Nickel oxide nanoparticles synthesis using plant extract and evaluation of their antibacterial effects on Streptococcus mutans, *Bioprocess and Biosystems Engineering*, **45(7)**, 1201-1210 **(2022)**

17. Narender S.S., Varma V.V.S., Srikar C.S., Ruchitha J., Varma P.A. and Praveen B.V.S., Nickel oxide nanoparticles: a brief review of their synthesis, characterization and applications, *Chemical Engineering & Technology*, **45(3)**, 397-409 **(2022)**

18. Noreen S. et al, Treatment of textile wastewater containing acid dye using novel polymeric graphene oxide nanocomposites (GO/PAN, GO/PPy, GO/PSty), *Journal of Materials Research and Technology*, **14**, 25-35 **(2021)**

19. Olajire A.A. and Mohammed A.A., Green synthesis of nickel oxide nanoparticles and studies of their photocatalytic activity in degradation of polyethylene films, *Advanced Powder Technology*, **31(1)**, 211-218 **(2020)**

20. Prabhu S., Thangadurai T.D., Bharathy P.V. and Kalugasalam P., Synthesis and characterization of nickel oxide nanoparticles using Clitoria ternatea flower extract: Photocatalytic dye degradation under sunlight and antibacterial activity applications, *Results in Chemistry*, **4**, 100285 **(2022)**

21. Regina Leong Zhi Ling, Sharon Kiung Tai Fhong, Lim Lai Huat, Su Shao Feng and Teo Swee Sen, Determination of antioxidant activity, chlorophyll and carotenoids content of Kappaphycus alvarezii: Comparison of seaweed with traditional Chinese Medicines, *Res. J. Biotech.*, **19(4)**, 24-31 **(2024)**

22. Selvanathan V. et al, Phytochemical-assisted green synthesis of nickel oxide nanoparticles for application as electrocatalysts in oxygen evolution reaction, *Catalysts*, **11(12)**, 1523 **(2021)**

23. Shahamat Y.D., Masihpour M., Borghei P. and Rahmati S.H., Removal of azo red-60 dye by advanced oxidation process O3/UV from textile wastewaters using Box-Behnken design, *Inorganic Chemistry Communications*, **143**, 109785 **(2022)**

24. Sharma P., Deep A., Kumar H., Chaudhary D., Thakur N. and Batra S., Qualitative analysis and anti-oxidant potential of ethanolic extract of Manilkara zapota (L.) P. Royen leaves, *Applied Drug Research, Clinical Trials and Regulatory Affairs*, **10(1)**, E290124226462 **(2024)**

25. Sharma S., Yadav D.K., Chawla K., Lal N., Alvi P.A. and Lal C., Degradation of dyes using biologically synthesized iron oxide nanoparticles by Manilkara zapota leaves extract, *Rasayan J Chem*, **15(3)**, 2165-2170 **(2022)**

26. Yadeta Gemachu L. and Lealem Birhanu A., Green synthesis of ZnO, CuO and NiO nanoparticles using Neem leaf extract and comparing their photocatalytic activity under solar irradiation, *Green Chemistry Letters and Reviews*, **17(1)**, 2293841 **(2024)**

27. Yashni G. et al, Bio-inspired ZnO NPs synthesized from Citrus sinensis peels extract for Congo red removal from textile wastewater via photocatalysis: Optimization, mechanisms, techno-economic analysis, *Chemosphere*, **281**, 130661 **(2021)**

28. Zafar Z., Fatima R. and Kim J.O., Experimental studies on water matrix and influence of textile effluents on photocatalytic degradation of organic wastewater using Fe–TiO2 nanotubes: Towards commercial application, *Environmental Research*, **197**, 111120 **(2021)**.

(Received 24th March 2025, accepted 15th May 2025)